

This is the accepted manuscript made available via CHORUS. The article has been published as:

Effect of selenium deficiency on the thermoelectric properties of n-type $\text{In}_{\{4\}}\text{Se}_{\{3-x\}}$ compounds

G. H. Zhu, Y. C. Lan, H. Wang, G. Joshi, Q. Hao, G. Chen, and Z. F. Ren

Phys. Rev. B **83**, 115201 — Published 4 March 2011

DOI: [10.1103/PhysRevB.83.115201](https://doi.org/10.1103/PhysRevB.83.115201)

The Effect of Selenium Deficiency on Thermoelectric Properties of n-type $\text{In}_4\text{Se}_{3-x}$ Compounds

G. H. Zhu¹, Y. C. Lan¹, H. Wang¹, G. Joshi¹, Q. Hao², G. Chen^{2*}, and Z. F. Ren^{1*}

¹*Department of Physics, Boston College, Chestnut Hill, Massachusetts 02467, USA*

²*Department of Mechanical Engineering, Massachusetts Institute of Technology, Cambridge, Massachusetts 02139, USA*

Abstract

Thermoelectric properties of dense bulk polycrystalline $\text{In}_4\text{Se}_{3-x}$ ($x = 0, 0.25, 0.5, 0.65$ and 0.8) compounds are investigated. A peak dimensionless thermoelectric figure-of-merit (ZT) of about 1 is achieved for $x = 0.65$ and 0.8 . The peak ZT is about 50% higher than the previously reported highest value for polycrystalline $\text{In}_4\text{Se}_{3-x}$ compounds. Our $\text{In}_4\text{Se}_{3-x}$ samples were prepared by ball milling and hot pressing. We show that it is possible to effectively control the electrical conductivity and thermal conductivity by controlling selenium (Se) deficiency x . The ZT enhancement is mainly attributed to the thermal conductivity reduction due to the increased phonon scattering by Se deficiency, defects and nanoscale inclusions in the ball milled and hot pressed dense bulk $\text{In}_4\text{Se}_{3-x}$ samples.

*To whom correspondence should be addressed: gchen2@mit.edu, renzh@bc.edu

Solid state energy conversion between heat and electricity based on thermoelectric effects has attracted extensive interest for many decades¹. Thermoelectric devices can be used for environmentally friendly refrigeration and power generation. The efficiency of thermoelectric devices is determined by a dimensionless thermoelectric figure-of-merit $ZT = (S^2\sigma/\kappa)T$, where S , σ , κ , and T are the Seebeck coefficient, electrical conductivity, thermal conductivity, and absolute temperature, respectively¹. Considerable effort has been made to improve the ZT values of the existing thermoelectric materials or to discover new high ZT materials. Recently, a noticeably high ZT was achieved in b - c plane of $\text{In}_4\text{Se}_{2.35}$ single crystals². In_4Se_3 crystallizes in a layered structure with weak van der Waals bonding between the layers along a axis and strong covalent bonding within the layer (b - c plane)^{2,3}. Due to charge density wave (CDW) and Peierls distortion, the thermal conductivity in b - c plane of bulk single crystal $\text{In}_4\text{Se}_{2.35}$ is greatly reduced². However, $\text{In}_4\text{Se}_{2.35}$ single crystals prepared by unidirectional crystal growth method, such as Bridgman technology, have remarkable anisotropy. Although $\text{In}_4\text{Se}_{2.35}$ is reported to have a ZT value of 1.48 at 432 °C in the b - c plane, the ZT value in the a - b plane is much lower, around 0.5 at 432 °C². Although polycrystalline $\text{In}_4\text{Se}_{3-x}$ compounds do not have anisotropy problem, the highest reported ZT is only about 0.6^{4,5}, which is not good enough for practical applications. In the past decade, numerous experimental and theoretical studies have shown that nanocomposite and nanostructuring approaches are effective in improving ZT ⁶⁻¹¹. In nanostructured systems, the enhanced ZT comes from a significant reduction in phonon thermal conductivity. Nanoscale grains and inclusions are believed to strongly scatter phonons which have relatively longer mean free paths than that of the electrons¹²⁻¹⁴. We note that In_4Se_3 single crystals have relatively high electrical resistivity, and the thermal conductivity mainly comes from the lattice thermal conductivity. Thus, we applied ball milling and hot pressing approach⁷⁻¹¹ to $\text{In}_4\text{Se}_{3-x}$ system, expecting to observe reduced lattice thermal conductivity due to the enhanced phonon scattering by nanograins and/or nanostructures in hot-pressed samples. Furthermore, different Se deficiency x in $\text{In}_4\text{Se}_{3-x}$ samples were prepared so as to optimize the thermoelectric properties.

In our work, different amounts of indium (In) and selenium (Se) elements were mixed together and pulverized into nanopowders by ball milling. All weighing and loading of the

materials were operated inside a glove box filled with argon gas. The nanopowders were hot pressed into discs by a quick direct current induced hot pressing process at 540 °C. X-ray diffraction (XRD, Bruker-AXS, D8), scanning electron microscopy (SEM, JEOL-6340F), and high resolution transmission electron microscopy (HRTEM, JEOL-2010F) were used to characterize the nanopowders and hot-pressed bulk samples. The electrical conductivity and Seebeck coefficient were measured simultaneously on the same bar samples of about $2 \times 2 \times 12$ mm in a multi probe transport system (Ulvac ZEM-3). The thermal diffusivity (α) was measured using a laser flash system (Netzsch LFA 457) and the heat capacity (C_p) was measured by a commercial differential scanning calorimeter (DSC 200 F3). The density of the hot-pressed samples was measured using an Archimedes' kit. The density of our hot pressed $\text{In}_4\text{Se}_{3-x}$ ($x = 0 - 0.8$) samples is $\sim 5.93 - 6.03 \text{ g cm}^{-3}$ that is very close to the theoretical value. The thermal conductivity κ is obtained as the product of thermal diffusivity (α), sample density (ρ), and heat capacity: $\kappa = \alpha\rho C_p$.

Fig. 1 shows the XRD spectrum of $\text{In}_4\text{Se}_{2.35}$ bulk samples after hot pressing. XRD pattern confirms that the major phase of our samples is In_4Se_3 phase. Since $\text{In}_4\text{Se}_{3-x}$ is thermodynamically unstable¹⁵, weak indium impurity phase was also detected in some of the $\text{In}_4\text{Se}_{3-x}$ samples.

Fig. 2 shows the transport properties of $\text{In}_4\text{Se}_{3-x}$ samples with different Se deficiency concentrations ($x = 0, 0.25, 0.5, 0.65$, and 0.8). The electrical resistivity ρ dependence of temperature as shown in Fig. 2(a), and the dependence of Se deficiency x , shown as the inset, indicate that the resistivity first decreases with increasing Se deficiency concentration up to $x = 0.5$, then increases with x . With increasing Se deficiency x from 0 to 0.8, $\text{In}_4\text{Se}_{3-x}$ samples change conducting behaviors: In_4Se_3 and $\text{In}_4\text{Se}_{2.2}$ are semiconductors whereas $\text{In}_4\text{Se}_{2.5}$ shows semimetallic behaviors, especially at around room temperature, with both hole and electron carriers, which results in a relatively lower electrical resistivity of $1.7 \times 10^{-4} \text{ ohm m}$ at room temperature. The effective carrier concentration n of $\text{In}_4\text{Se}_{2.5}$, measured by using the van der Pauw method¹⁶, is $1.68 \times 10^{18} \text{ cm}^{-3}$ at 25 °C, almost two orders of magnitude higher than $4.02 \times 10^{16} \text{ cm}^{-3}$ (In_4Se_3) and $4.13 \times 10^{16} \text{ cm}^{-3}$ ($\text{In}_4\text{Se}_{2.2}$). The mobility of $\text{In}_4\text{Se}_{3-x}$ samples varies from $29.1 \text{ cm}^2 \text{ V}^{-1} \text{ S}^{-1}$ ($\text{In}_4\text{Se}_{2.5}$) to $189 \text{ cm}^2 \text{ V}^{-1} \text{ S}^{-1}$ (In_4Se_3), which is lower than the reported value⁴. The relatively low mobility in our $\text{In}_4\text{Se}_{3-x}$ samples is mainly due to the

increased scattering of the charge carriers by the increased number of grain boundaries and defects in our ball milled and hot pressed samples.

Large negative Seebeck coefficient values are observed in $\text{In}_4\text{Se}_{2.2}$, $\text{In}_4\text{Se}_{2.35}$ and In_4Se_3 samples (Fig. 2(b)). Semiconducting $\text{In}_4\text{Se}_{2.2}$ sample shows a maximum Seebeck coefficient of about $-560 \mu\text{VK}^{-1}$ at room temperature, whereas semimetallic $\text{In}_4\text{Se}_{2.5}$ sample shows the lowest Seebeck coefficient of $-26 \mu\text{VK}^{-1}$ at room temperature due to the existence of both types of carriers. The thermoelectric power factor ($S^2\sigma$) is shown in Fig. 2(c). Because of the low electrical transport properties, $S^2\sigma$ values are small for all $\text{In}_4\text{Se}_{1-x}$ samples.

Fig. 2(d) and 2(e) show the temperature dependence of the thermal conductivity κ and dimensionless figure-of-merit ZT . As shown in Fig. 2(d), the thermal conductivity κ decreases from $0.75 \text{ Wm}^{-1}\text{K}^{-1}$ to $0.41 \text{ Wm}^{-1}\text{K}^{-1}$ at 425°C with increasing temperature for $\text{In}_4\text{Se}_{2.2}$ that has the lowest thermal conductivity among all samples, which is about 40% lower than the reported value in the polycrystalline $\text{In}_4\text{Se}_{3-x}$ compounds⁴. The low thermal conductivity in our $\text{In}_4\text{Se}_{3-x}$ samples should be attributed to the defect induced phonon scattering by the Se deficiency sites and enhanced phonon scattering due to the higher grain boundary density. Fig. 2(e) shows the thermal diffusivity and specific heat capacity values of $\text{In}_4\text{Se}_{3-x}$ samples. Very low diffusivity values are observed in all $\text{In}_4\text{Se}_{3-x}$ samples and the diffusivity decreases with increasing Se deficiency in high temperature region, indicating strong phonon scattering by Se vacant sites. ZT (Fig. 2(f)) increases with temperature and reaches the maximum value at 425°C . Owing to the significantly reduced thermal conductivity, the hot pressed $\text{In}_4\text{Se}_{3-x}$ samples exhibit peak ZT values of 0.97 and 0.96 at 425°C for $\text{In}_4\text{Se}_{2.2}$ and $\text{In}_4\text{Se}_{2.35}$ samples, respectively.

In order to understand the mechanism of the thermal conductivity reduction and ZT enhancement in the hot pressed $\text{In}_4\text{Se}_{3-x}$ samples, preliminary TEM studies were carried out. The TEM specimens were prepared by both focused ion beam (FIB) using standard H-bar method and mechanical polishing down to several microns using tripod, then Ar^+ ion-milling using Gatan PIPS. Unfortunately it turned out that the sample preparation is very challenging, the specimens were very easily contaminated. It seems that the contamination was caused by the materials decomposition and re-crystallization on the specimen surface during the FIB

and ion-milling process. Fig. 3(a) shows a typical TEM image of the ion-milled TEM specimens for $\text{In}_4\text{Se}_{2.2}$ from which we can clearly see that the average grain size is about 400 – 700 nm (Fig. 3(a)), due to the grain growth during the hot pressing process. Although the grain size is much smaller than the conventional polycrystalline compounds, they are still too big to effectively scatter phonons and cannot be the reason to explain the low thermal conductivity in Fig. 2(d). In order to study the microstructures of the grains by HRTEM, a clean specimen was carefully mechanically polished to electron transparent by tripod without using Ar^+ ion-mill to prevent contamination. The TEM specimen prepared in such a way is clean without any contamination, but the area which is thin enough for TEM is rather small. HRTEM of the $\text{In}_4\text{Se}_{2.2}$ specimen (Fig. 3(b)) shows that there are some nanoscale features of sizes up to 10 nm inside the grains. The energy dispersive X-ray spectroscopy (EDS) result shows that the nanoscale inclusions have the same composition with the nearby matrix within EDS experimental error (± 1 atm %). Moreover, we also noticed that there are many dislocations and point defects in our hot pressed samples. In order to investigate the dislocations in the specimens, the fast-Fourier-transform (FFT) of HRTEM images are generated using the DigitalMicrograph software (Gatan Inc., PA). A series of inverse Fast-Fourier-Transferred (IFFT) images are reconstructed from mask-applied FFT of HRTEM images. The dislocations distinguished as lattice discontinuities are directly observed from these reconstructed IFFT images. The estimated dislocation density (N_D) is higher than 10^{12} cm^{-2} . The relatively low mobility measured in the hot pressed $\text{In}_4\text{Se}_{3-x}$ samples should be resulted from the high density of dislocations and point defects. We believe that the increased grain boundary density, line dislocation density, nanoscale inclusions, and, especially, the Se vacant sites all contribute to the reduced phonon thermal conductivity κ_{ph} .

A couple of interesting things need to be pointed out for this material system: 1) the electrical conductivity in the range of 2×10^2 to $6 \times 10^3 \text{ Sm}^{-1}$ is too low for the materials to be good thermoelectric materials with very high ZT so there is a large room for improvement in ZT if a suitable dopant can be found to significantly increase the electrical conductivity without too much affecting the Seebeck coefficient, and 2) the conducting behavior change from semiconducting to semimetallic with the Se deficiency deserves further detailed studies.

Conclusion

Dense bulk $\text{In}_4\text{Se}_{3-x}$ samples with different Se deficiencies were prepared by ball milling and hot pressing. Semimetallic behavior was observed when the Se deficiency x is close to 0.5. High Se deficiency ($x = 0.65$ and 0.8) doesn't deteriorate the electrical properties, but rather reduces the thermal conductivity, resulting in improved ZT values. A peak ZT of about 1 is achieved in $\text{In}_4\text{Se}_{2.2}$ at 425°C , which is about 50% higher than the previously reported highest value for polycrystalline samples. This ZT enhancement mainly comes from the reduction of thermal conductivity due to the increased phonon scattering by high Se deficiency, defects and nanoscale inclusions.

Acknowledgment: The work is funded by the US Department of Energy under contract number DOE DE-FG02-00ER45805 (ZFR), and Solid State Solar-Thermal Energy Conversion Center (S^3TEC), an Energy Frontier Research Center funded by the U.S. Department of Energy, Office of Science, Office of Basic Energy Sciences under Award Number: DE-SC0001299 (G.C. and Z.F.R.).

- ¹C. Wood, Rep. Prog. Phys. **51**, 459 (1988).
- ²J. Rhyee, K. H. Lee, S. M. Lee, E. Cho, S. I. Kim, E. Lee, Y. S. Kwon, J. H. Shim, and G. Kotliar, Nature (London) **459**, 965 (2009).
- ³Y. B. Losovyj, M. Klinke, E. Cai, I. Rodriguez, J. Zhang, L. Makinistian, A. G. Petukhov, E. A. Albanesi, P. Galiy, Y. Fiyala, J. Liu, and P. A. Dowben, Appl. Phys. Lett. **92**, 122107 (2008).
- ⁴J. Rhyee, E. Cho, K. H. Lee, S. M. Lee, S. I. Kim, H. Kim, Y. S. Kwon, and S. J. Kim, Appl. Phys. Lett. **95**, 212106 (2009).
- ⁵X. Shi, J. Y. Cho, J. R. Salvador, J. Yang, and H. Wang, Appl. Phys. Lett. **96**, 162108 (2010).
- ⁶K. F. Hsu, S. Loo, F. Guo, W. Chen, J. S. Dyck, C. Uher, T. Hogan, E. K. Polychroniadis, and M. G. Kanatzidis, Science **303**, 818 (2004).
- ⁷B. Poudel, Q. Hao, Y. Ma, Y. C. Lan, A. Minnich, B. Yu, X. Yan, D. Z. Wang, A. Muto, D. Vashaee, X. Chen, J. M. Liu, M. S. Dresselhaus, G. Chen, and Z. F. Ren, Science **320**, 634 (2008).
- ⁸Yi Ma, Qing Hao, Bed Poudel, Yucheng Lan, Bo Yu, Dezhi Wang, Gang Chen, and Z. F. Ren, *NanoLetters* **8**, 2580 – 2584 (2008).
- ⁹G. Joshi, H. Lee, Y. C. Lan, X. W. Wang, G. H. Zhu, D. Z. Wang, A. J. Muto, M. Y. Tang, M. S. Dresselhaus, G. Chen, and Z. F. Ren, Nano Lett. **8**, 4670 (2008).
- ¹⁰X. W. Wang, H. Lee, Y. C. Lan, G. H. Zhu, G. Joshi, D. Z. Wang, J. Yang, A. J. Muto, M. Y. Tang, J. Klatsky, S. Song, M. S. Dresselhaus, G. Chen, and Z. F. Ren, Appl. Phys. Lett. **93**, 193121 (2008).
- ¹¹G. H. Zhu, H. Lee, Y. C. Lan, X. W. Wang, G. Joshi, D. Z. Wang, J. Yang, D. Vashaee, H. Guilbert, A. Pillitteri, M. S. Dresselhaus, G. Chen, and Z. F. Ren, Phys. Rev. Lett. **102**, 196803 (2009).
- ¹²G. Chen, Semiconductors and Semimetals, **71**, 203 (2001).
- ¹³M. S. Dresselhaus, G. Chen, Z. F. Ren, J. P. Fleurial, and P. Gogna, Adv. Mater. **19**, 1043 (2007).
- ¹⁴A. Majumdar, Science **303**, 777 (2004).
- ¹⁵H. Okamoto, Journal of Phase Equilibria and Diffusion **25(2)**, 201, (2004).
- ¹⁶C. Wood, A. Lockwood, A. Chmielewski, J. Parker, and A. Zoltan, Rev. Sci. Instrum. **55**,

110 (1984).

Figure Captions:

FIG. 1. XRD spectrum of dense bulk samples $\text{In}_4\text{Se}_{2.35}$ after hot pressing.

FIG. 2. Temperature-dependent electrical resistivity (a), Seebeck coefficient (b), power factor (c), thermal conductivity (d), specific heat C_p and diffusivity (e) and ZT (f) of hot pressed dense bulk samples $\text{In}_4\text{Se}_{3-x}$. The inset in (a) shows the electrical resistivity dependence of Se deficiency.

FIG. 3. (a) Low magnification TEM image of the typical hot pressed $\text{In}_4\text{Se}_{3-x}$ samples and (b) nanoscale inclusions found in high resolution images.

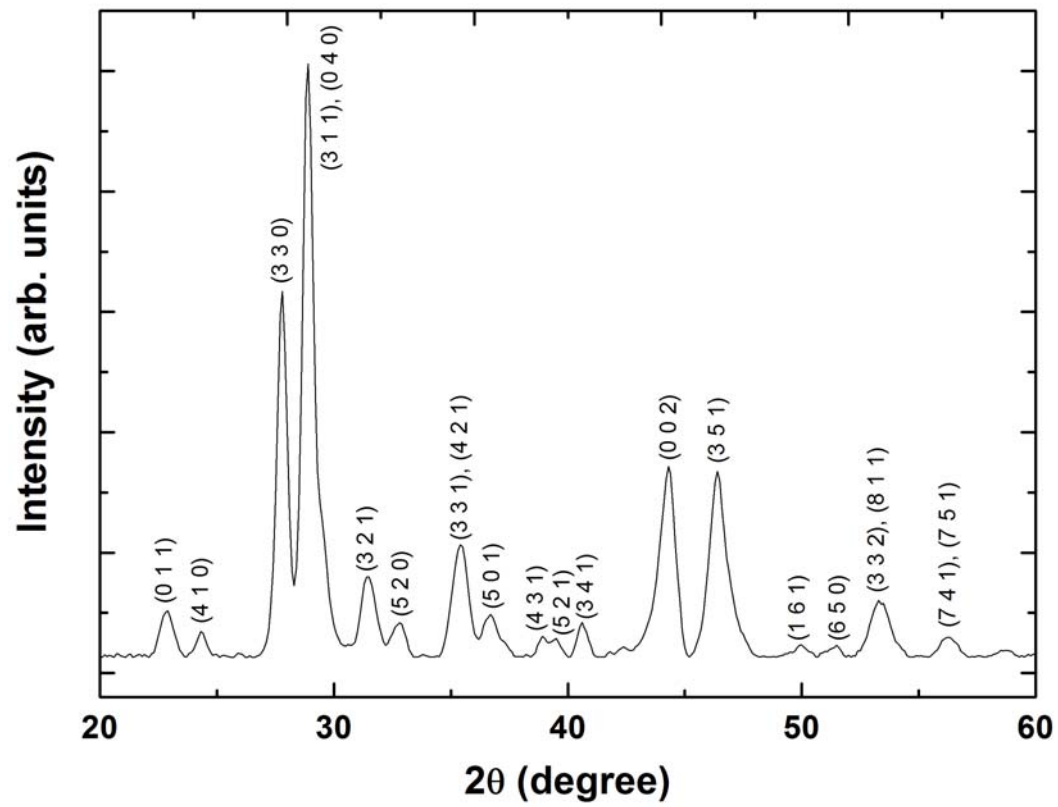


FIG. 1, G. H. Zhu *et al.*

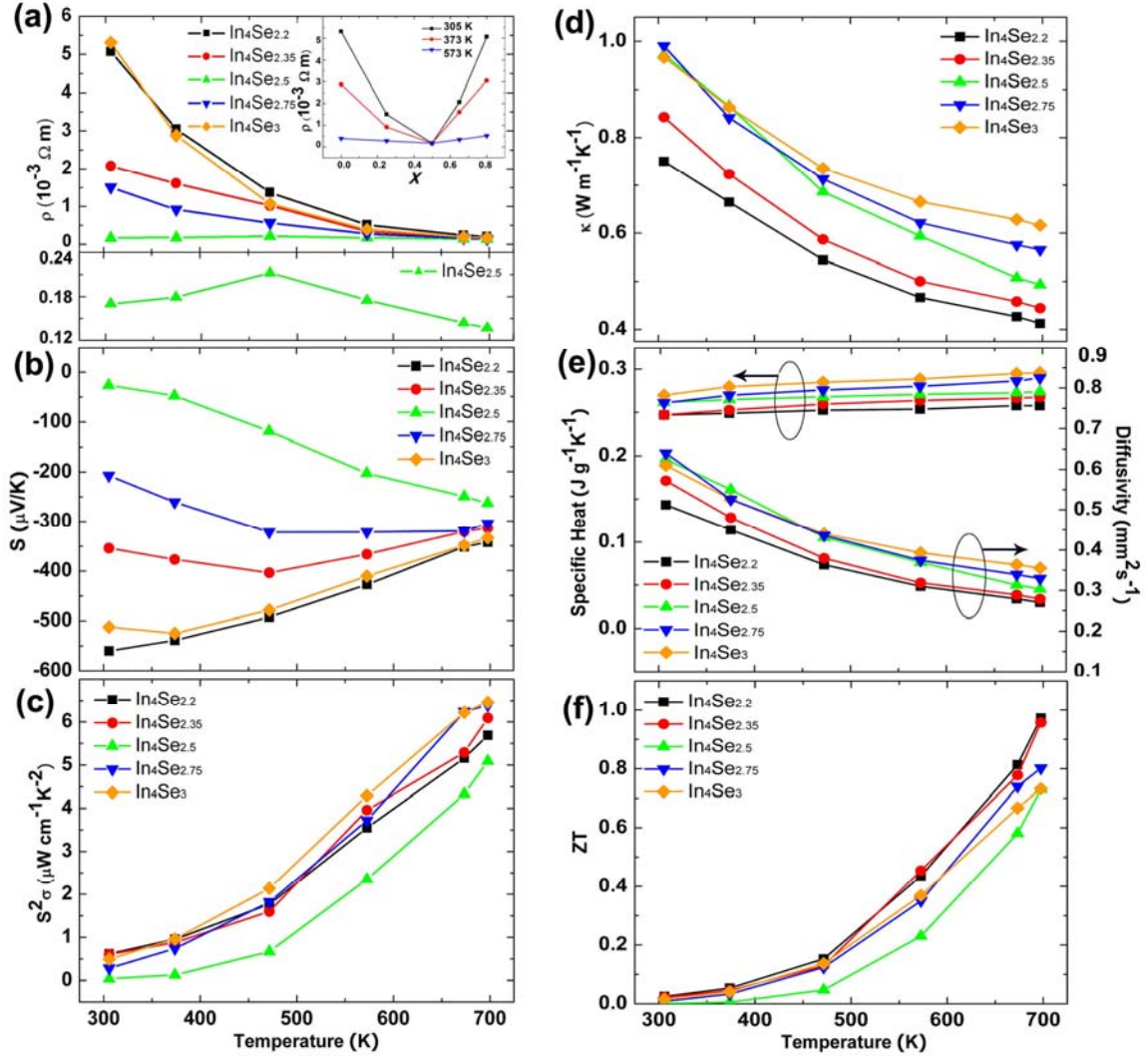


FIG. 2, G. H. Zhu *et al.*

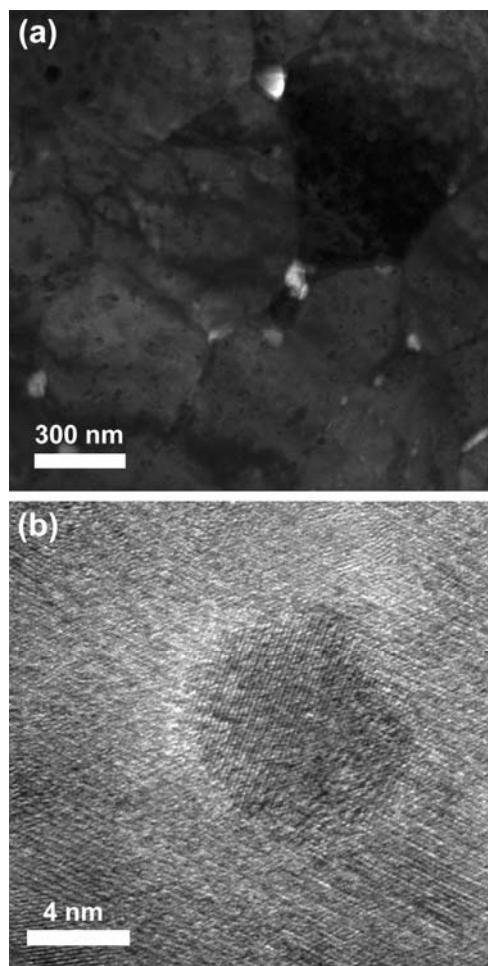


FIG. 3, G. H. Zhu *et al.*